Biomixing due to diel vertical migrations of zooplankton: Comparison of computational fluid dynamics model with observations

Article *in* Ocean Modelling · December 2015

DOI: 10.1016/j.ocemod.2015.12.002

CITATIONS
5

READS
233

5 authors, including:

Cayla Dean
Nova Southeastern University
13 PUBLICATIONS **18** CITATIONS
SEE PROFILE

A. Soloviev
Nova Southeastern University
112 PUBLICATIONS **1,694** CITATIONS
SEE PROFILE

Amy Hirons
Nova Southeastern University
17 PUBLICATIONS **304** CITATIONS
SEE PROFILE

Tamara Frank
Nova Southeastern University
48 PUBLICATIONS **1,144** CITATIONS
SEE PROFILE

Ocean Modelling 98 (2016) 51–64

Contents lists available at ScienceDirect

Ocean Modelling

journal homepage: www.elsevier.com/locate/ocemod

Virtual Special Issue
GoM Virtual Special Issue

Biomixing due to diel vertical migrations of zooplankton: Comparison of computational fluid dynamics model with observations

Cayla Dean[a,*], Alexander Soloviev[a,b], Amy Hirons[a], Tamara Frank[a], Jon Wood[c]

[a] Nova Southeastern University Oceanographic Center, 8000 North Ocean Drive, Dania Beach, FL 33004, United States
[b] Rosenstiel School of Marine and Atmospheric Science, University of Miami, 4600 Rickenbacker Causeway, Miami, FL 33149, United States
[c] Ocean Data Technologies, Inc., 153 Lovells Lane Suite C, Marstons Mills, MA 02648, United States

ARTICLE INFO

Article history:
Received 5 April 2015
Revised 25 November 2015
Accepted 8 December 2015
Available online 17 December 2015

Keywords:
Diel vertical migrations (DVM)
Zooplankton
Computational fluid dynamics
Modeling
Turbulence

ABSTRACT

Recent studies (Dewar et al., 2006; Wilhelmus and Dabiri, 2014) suggest that diel vertical migrations (DVM) of zooplankton (or other migrating organisms) may have an impact on ocean mixing, though details are not completely clear. Zooplankton that undergo DVM can have an impact on oil transport through the water column, and oil and dispersants can have a negative or even lethal effect on the organisms. Kunze et al. (2006) reported an increase of dissipation rate of turbulent kinetic energy, ε, by four to five orders of magnitude during DVM of zooplankton over background turbulence in Saanich Inlet, British Columbia, Canada. However, the effect was not observed in the same area by Rousseau et al. (2010) and was later reassessed by Kunze (2011). In our work, an 11-month data set obtained in the Straits of Florida with a bottom-mounted acoustic Doppler current profiler revealed strong sound scattering layers undergoing DVM. We used a 3-D non-hydrostatic computational fluid dynamics model with Lagrangian particle injections (a proxy for migrating organisms) via a discrete phase model to simulate the effect of turbulence generation by DVM. We tested a range of organism concentrations from 1000 to 10,000 organisms/m^3 based on measurements by Greenlaw (1979) and Mackie and Mills (1983) in Saanich Inlet. At a concentration close to the upper limit, the simulation showed an increase in ε by two to three orders of magnitude during DVM over background turbulence, 10^{-9} W kg^{-1}. At a concentration of 1000 organisms/m^3, almost no turbulence above the background level was produced in the model. These results suggest that the Kunze et al. (2006) observations could have been performed at a larger concentration of migrating zooplankton than those reported by Rousseau et al. (2010). No exact zooplankton concentrations data were provided in either work. The difference between observations and the model can, in part, be explained by the fact that Kunze et al. (2006) measured instantaneous profiles of ε, while the model results on ε were averaged horizontally over the 50 m by 50 m domain. In the Straits of Florida, we observed a small decrease in northward current velocity profiles during migration times after averaging over 11 months of observations. The computational fluid dynamics model reproduced this decrease of current velocity due to turbulence generated by DVM in the Straits of Florida model case. The deviations in the velocity profiles can be explained by the increase in turbulent mixing during vertical migration periods. Comparison of observational data to the model results was complicated by physical factors such as tides, Florida Current meandering, etc., which may have a stronger effect on current velocity profiles than DVM.

1. Introduction

The Deepwater Horizon oil spill disaster began on April 20, 2010, and continued to discharge oil until September 19, 2010, spilling approximately 210 million US gallons, making it the largest accidental marine oil spill in history (Crone and Tolstoy, 2010). The impact on marine ecosystems is still under evaluation by the Gulf of Mexico Research Initiative (Carassou et al., 2014). Zooplankton comprise one of the largest groups of organisms in the upper ocean with very high diversity and biomass. Remarkably, zooplankton that undergo diel vertical migration (DVM) can have an impact on oil transport through the water column and oil can have a negative effect on the health of the organisms. Cohen et al. (2014) assessed lethal and non-lethal effects of oil and dispersant toxicity on zooplankton. This work provides an important insight in the problem of DVM of zooplankton in the presence of an oil spill. The study of DVM of zooplankton can help in

* Corresponding author. Tel.: +1 865 254 4098/954 262 3636.
E-mail address: cd821@nova.edu, statlab201@gmail.com (C. Dean).

http://dx.doi.org/10.1016/j.ocemod.2015.12.002
1463-5003/

understanding how marine ecosystems in the Gulf of Mexico respond to oil spill events.

Ianson et al. (2004) proposed, from conservative assumptions, that approximately 15% of zooplankton biomass undergo DVM, composing the largest animal migration on the planet (Andersen et al., 1991). DVM typically occurs at sunrise and sunset, with changes in light thought to initiate synchronization of upward/downward motion and determine the rate of ascent/decent (Haney, 1988). The hypothesis that has received the strongest experimental validation regarding the ultimate cause of DVM is predator avoidance. The predator avoidance hypothesis states that adoption of migratory or non-migratory behaviors is based on the relative abundance of visual orienting predators, food, and level of satiation (Gliwicz, 1986; Lampert, 1989; De Robertis et al., 2003). The concentration of food at depth is not adequate to meet energy requirements of many organisms; therefore, migration to the near surface waters is necessary to meet these demands (Stich and Lampert, 1981). Predators are more likely to see their prey during the day, leading to zooplankton occupation of darker, deeper water during the day and ascent to the surface waters during the evening (Enright, 1977).

Recent studies (Dewar et al., 2006; Wilhelmus and Dabiri, 2014) suggest that DVM of zooplankton may have an impact on ocean mixing. Munk (1966) first suggested that biological mixing (biomixing) may contribute to the ocean energy budget to some extent. On a global scale, biomixing implies that swimming organisms vertically transport colder water from the deeper layers toward the surface and warm water from the near surface waters to the deeper layers, thereby affecting the global ocean circulation (Dewar et al., 2006). These organisms may transport anthropogenic pollutants through the water column. DVM could also contribute to gas exchange between the ocean and atmosphere, thereby playing a role in the carbon cycle and climate (Kunze et al., 2006). On a local scale, DVM can explain higher levels of surface production (Jenkins and Doney, 2003). Higher levels of surface primary productivity may be due to schools of organisms migrating through the thermocline and transporting nutrient-rich water upward in the water column, increasing the possibility of phytoplankton growth. However, these organisms could be larger than zooplankton in order to provide sufficient mixing efficiency (Huntley and Zhou, 2004; Visser, 2007).

Wunsch and Ferrari (2004) and St. Laurent and Simmons (2006) estimated that 2 to 3 terawatts (TW) of power is required to sustain global ocean circulation. If only waves and tides are considered, there is a deficit of approximately 1 TW in the ocean energy budget (Munk and Wunsch, 1998; Wunsch, 2000). The oceanic biosphere captures approximately 63 TW of solar energy, and while only a small percentage is converted to the mechanical energy of swimming, this may fill the gap in the energy budget (Dewar et al., 2006). Visser (2007) and Kunze (2011), however, later expressed doubts about this hypothesis due to relatively small-scale turbulence and, possibly, negligible contribution to mixing efficiency by migrating individual organisms. An alternative point of view is that there is no deficit in the global mixing budget when patchiness of diapycnal mixing in space and time is taken into account (Waterhouse et al., 2014).

Velocity fluctuations from motion at relatively small scales are known to cause swimming-induced turbulence (Huntley and Zhou, 2004). Laboratory studies confirmed that schools of swimming animals create measurable increases in fluid disturbances (Catton et al., 2011; Wilhelmus and Dabiri, 2014). Evaluations based on energetics of swimming organisms indicate that organisms ranging from large zooplankton (0.5 cm) to cetaceans (10 m) can generate dissipation rates of turbulent kinetic energy (ε) on the order of 10^{-5} W kg^{-1} in schools and swarms (Huntley and Zhou, 2004; Dewar et al., 2006), which is three to four orders of magnitude larger than average ε in a stratified ocean. This local energy dissipation is comparable to ε associated with major storms and may potentially provide an additional source of fine-scale turbulent mixing (MacKenzie and Leggett, 1993).

Observations by Kunze et al. (2006) indicated a localized increase in ε of four to five orders of magnitude in the wake of a school of migrating krill. While this DVM was short in duration, it led to an increase in daily-averaged turbulent eddy diffusivities by two to three orders of magnitude. Subsequent discussion (Kunze et al., 2007) suggested that shear fluctuations at length scales much larger than the individual organism could develop (provided that krill acted as a unit rather than individuals). In aggregations of swimming organisms, turbulence does not have time to decay before being encountered by another organism causing an increase of turbulence length and temporal scales (Gregg and Horne, 2009). The net ε due to a school of swimming organisms depends on the power expended per individual and the number of individuals per unit volume (Dewar et al., 2006). For a school of krill with body lengths of approximately 1.5 cm, swim speeds of 5 to 10 cm s^{-1}, and density of individuals of about 5000 organisms m^{-3}, ε is approximately 10^{-5} to 10^{-4} W kg^{-1} (Huntley and Zhou, 2004), which is consistent with the observations from Kunze et al. (2006). This behavior has also been shown using modeling techniques. Dabiri (2010) used a simple rigid body model and observed overturning length scales larger than the individual animals during vertical movement of the entire aggregation.

Our work aims to model the effect of zooplankton DVM on turbulence signature and velocity profile. First, we collected and analyzed acoustic and velocity data involving DVM for the Straits of Florida and used a 3-D non-hydrostatic computational fluid dynamics model to observe the effect of zooplankton DVM. Second, we attempted to reproduce the observed increase of ε due to DVM of zooplankton observed by Kunze et al. (2006) in Saanich Inlet, British Columbia, Canada using a similar model. A better understanding of the effects of DVM on upper ocean dynamics is expected to help in solving the more complex problem involving transport of anthropogenic pollutants including dissolved oil in the water column in future research. The structure of the paper is as follows. Observations in the Straits of Florida are described in Section 2. The computational fluid dynamics setup is described in Section 3. Results are presented in Section 4, discussion in Section 5, and conclusions in Section 6.

2. Measurements in the Straits of Florida

We collected acoustic data with a bottom mounted Teledyne RD Instruments acoustic Doppler current profiler (ADCP) Workhorse Longranger 75 kHz (Fig. 1) located in the Straits of Florida off Dania Beach, FL at a 244 m depth isobath close to the edge of the Gulf

Fig. 1. The mooring equipped with Teledyne RDI ADCP (Workhorse Longranger 75 kHz).

Stream (26.0315°N, 79.9937°W) (Soloviev et al., 2015). Data collection occurred every 5 min from December 16, 2010, at 11:00 GMT until October 11, 2011, at 14:30 GMT (Fig. 2). Note that the bins corresponding to the upper 28 m have been removed from the record due to multiple reflections from the ocean surface. Sunrise and sunset times were collected from http://aa.usno.navy.mil/cgi-bin/aa_rstablew.pl, and wind speed and direction were obtained from the National Oceanic and Atmospheric Administration's National Data Buoy Center (NOAA NDBC) at the Fowey Rock station to assist with ADCP data analysis.

Acoustic data from the ADCP provided an understanding of some of the major features of the Florida Current. The contour plot in Fig. 3 clearly shows the presence of a strong western boundary current, the Florida Current. The velocity variations due to meandering were quite prominent because the ADCP mooring was deployed in the vicinity of the Gulf Stream front. Temporal periodicity of the current velocity due to the tidal cycle is also noticeable. These data provided information on the physical oceanographic conditions in the study area and helped to initialize the velocity profile in the computational fluid dynamics model.

At 75 kHz, the ADCP responds to particles or aggregates 8 mm or larger, which could represent large individual zooplankton, swarms of zooplankton, or small fish. The contour plot of backscatter signal from the ADCP clearly shows a periodic pattern. Higher backscatter in the surface water is directly followed by higher backscatter in mid-depths throughout most of the data set, suggesting the presence of a DVM cycle (Fig. 4). To observe if this was DVM, we overlaid sunrise and sunset times on the same plot. Sunrise is indicated by a solid white line, sunset as a dashed white line, new moon as a solid black line, and full moon as a dashed black line (Fig. 5). Sunset and sunrise times clearly coincided with the changes in backscatter signal in the upper ocean. Within an hour of sunset, in almost all cases, the backscatter intensity was much stronger at the surface than before sunset indicating an upward migration. Within 45 min of sunrise, the higher backscatter intensity at the surface had almost disappeared, indicating a downward migration. DVM patterns due to lunar cycle were not analyzed for this work. It should be emphasized that in general DVM does not correlate in time with the tidal cycle.

We obtained an estimate of the abundance of zooplankton at the ADCP location from the data collected during a previous observational period at a location with similar depth and distance offshore, approximately 20 miles downstream (USCG, 2008). We expect the concentrations obtained at the location 20 miles downstream to be similar to our study site since both sites are located in the Gulf Stream. The backscatter measurements from the ADCP also did not show any principle differences in concentration patterns between these locations. The previous study collected zooplankton and ichthyoplankton samples via two bongo nets with 202 μm and 335 μm mesh and one Tucker trawl net with 760 μm mesh to identify species present at deep water sites within the Straits of Florida. These nets were used to collect daytime and nighttime samples at shallow (25 m) and deep (200 m) depths. Data from the nets provided taxa composition, size range of organisms, typical swimming velocities, and typical zooplankton density/biomass in day versus night samples. However, net avoidance behavior is well known, especially for larger species, leading to underestimates of zooplankton concentrations (Pakhomov and Yamamura, 2010). As a result, we have explored a range of zooplankton concentrations in the computational fluid dynamics experiment.

The Southeast Florida shelf is a very energetic zone due to the presence of a major western boundary current. To observe possible effect on current velocity due to DVM, we averaged 11 months of the northward current velocity measurements of the Florida Current during migration times over 120 min, starting 60 min before and ending 60 min after sunrise or sunset, and compared these data with 120 min corresponding averages from three hours prior to the migration times. Only cases when the core of the Florida Current was present above the mooring, identified by northward velocity greater than 0.75 m s^{-1}, were considered. A 95% confidence interval was then calculated for the average northward velocity profiles.

Averaging over a long time period is expected to suppress the variability that is not coherent with the diel cycle. Daily cycles in physical forces such as winds and heating can shift abruptly at sunrise and sunset. However, it takes some time for these factors to propagate within the water column, and it is not clear if they affect the turbulence regime below relatively shallow near surface layers.

3. Computational fluid dynamics model

Our work utilized ANSYS *Fluent*, a commercial computational fluid dynamics (CFD) modeling software, to simulate the effect of DVM on small scale turbulence the best we can with the resolution afforded, given the physics prescribed in the model parameterizations.

The simulations considered two locations, Saanich Inlet and the Straits of Florida. We first modeled the Saanich Inlet field data in an attempt to replicate the effects of DVM on ε observed by Kunze et al. (2006) during sunset migration. For this case, the domain was a 50 m by 50 m by 150 m box representing a section of Saanich Inlet, British Columbia, Canada (Fig. 6a). The Straits of Florida case aimed to determine if an increase of ε is present and if there was any effect on the current velocity profile. For this case, the domain was a 50 m by 50 m by 250 m box representing a section of the Straits of Florida (Fig. 7a). Both domains had a one-meter resolution mesh in all three directions.

For each model run, acceleration due to gravity and the energy equation were included. Large Eddy Simulation/Wall Adapting Local Eddy Viscosity Model (LES WALE) was used to model turbulence (see Appendix A). It should be noted that LES has a somewhat artificial length scale separation between explicitly modeled and subgrid components.

To be sure of adequate mesh resolution, we have performed a validation test for mesh resolutions 2 m, 1 m, and 0.5 m. We did see some difference between 2 m and 1 m resolutions, but not a significant difference between 1 m and 0.5 m resolutions. Our simulations were conducted using 1 m resolution, which we assumed to be adequate for this purpose.

Boundary conditions for both the Saanich Inlet and the Straits of Florida cases were set in the following way. We imposed periodic boundary conditions at the inlet and outlet to allow infinite fetch and to allow particles (simulating zooplankton migration) to remain in the domain indefinitely. We set the bottom boundary condition to a no-slip condition and the sides of the domain at 0 specified shear (which is equivalent to slippery boundary conditions). We set the top boundary condition to 0.048 Pa corresponding to approximately 5 m s^{-1} wind (a typical wind speed at this location according to the nearby NOAA weather station, Fowey Rock). We set the heat flux at the top boundary at 20 W m^{-2} immediately before sunset and -100 W m^{-2} during sunset.

Both cases of the model used a pressure-based solver with the SIMPLE scheme for pressure-velocity coupling. For spatial discretization, PRESTO! Scheme was used for pressure (ANSYS *Fluent*, 2013); a Least Squares Based scheme was used for gradient; Bounded Central Difference for momentum; and Second Order Upwind for energy. The time-stepping scheme was set to Second Order Implicit. The material properties were set to that of pure water with density specified as a polynomial dependent on temperature.

The model was initialized with idealized density and velocity profiles (Figs. 6b, c and 7b, c). For the Saanich Inlet case, stratification information was taken from temperature and salinity profiles averaged over several days of sample collection (Rousseau et al., 2010). Current velocity profiles were not available for this specific location so it was estimated from the VENUS observatory in the Strait of Georgia, which is just outside of Saanich Inlet (http://venus.uvic.ca/).

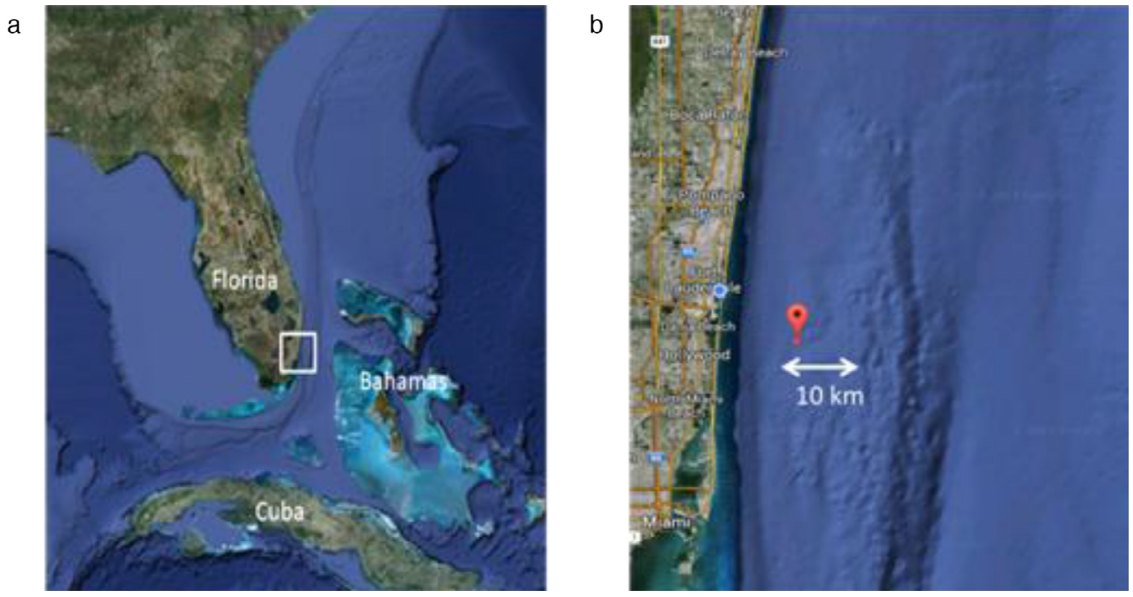

Fig. 2. Map of the site where instruments were located: (a) large scale area where the study was conducted; (b) magnified white box from (a).

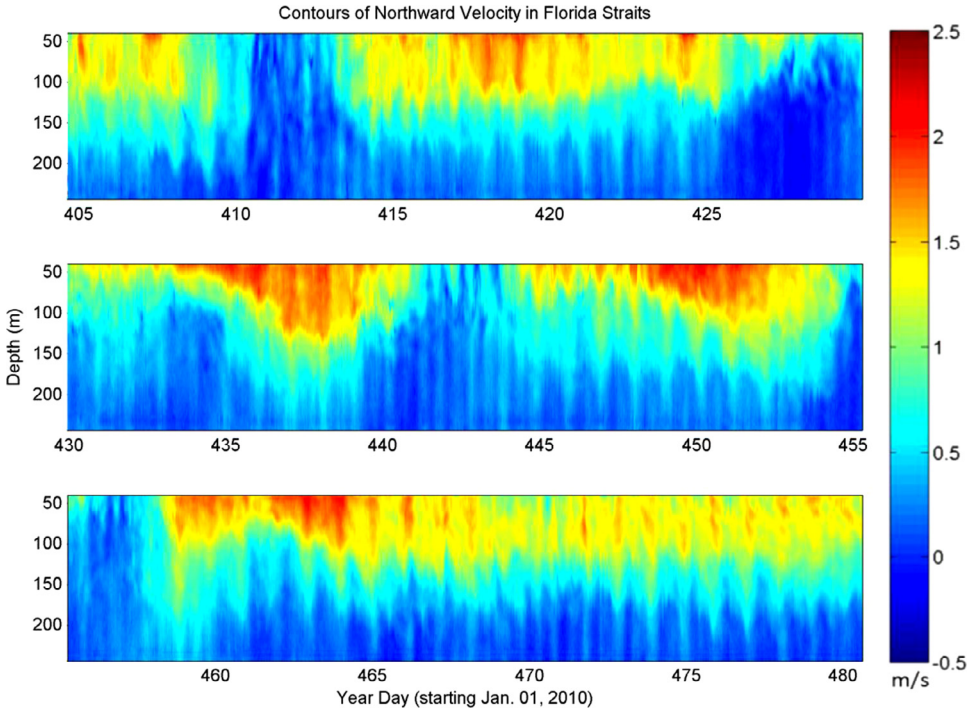

Fig. 3. Northward current velocity contour plots for a subset of the 11 month data set from February 9, 2011 to April, 26, 2011. Near surface bins corresponding to 28 m have been removed due to multiple reflections.

For the Straits of Florida case, observational velocity profiles were used (Fig. 7c). The temperature/salinity structure was estimated from historical data, constrained by SAIC (1992) and near-bottom temperature from ADCP and sea surface temperature from the NDBC buoy at Fowey Rock (Fig. 7b).

To model zooplankton, particles were injected into the domain using a discrete phase model (DPM) to simulate DVM cycles (ANSYS *Fluent*, 2013). The buoyancy of particles was adjusted by setting the density of rigid spherical particles 1.2% less dense than the water at the plane of injection (100 m), allowing the particles to float toward the surface with several cm s^{-1} vertical speed. The spherical drag law was set to approximate drag of the particles. The drag coefficient, C_D, for spherical particles is defined by

$$C_D = \alpha_1 + \frac{\alpha_2}{\mathrm{Re}} + \frac{\alpha_3}{\mathrm{Re}^2}$$

where α_1, α_2, and α_3 are constants over several ranges of Reynolds number (Morsi and Alexander, 1972). Here the Reynolds number for the particles was approximately 550 as reported by the *Fluent* model. From the density difference, Reynolds number and the drag law, it was possible to calculate terminal velocity as follows.

$$V_t = \sqrt{\frac{4gd}{3C_D}\left(\frac{\rho_s - \rho}{\rho}\right)}$$

The terminal velocity was approximately 5 cm s^{-1} which is comparable to swimming velocities reported by Kunze et al. (2006).

DPM allows simulation of a discrete second phase in a Lagrangian frame of reference. This dispersed phase consisted of spherical particles dispersed in the continuous phase (fluid). *Fluent* computes particle trajectories individually during the hydrodynamic

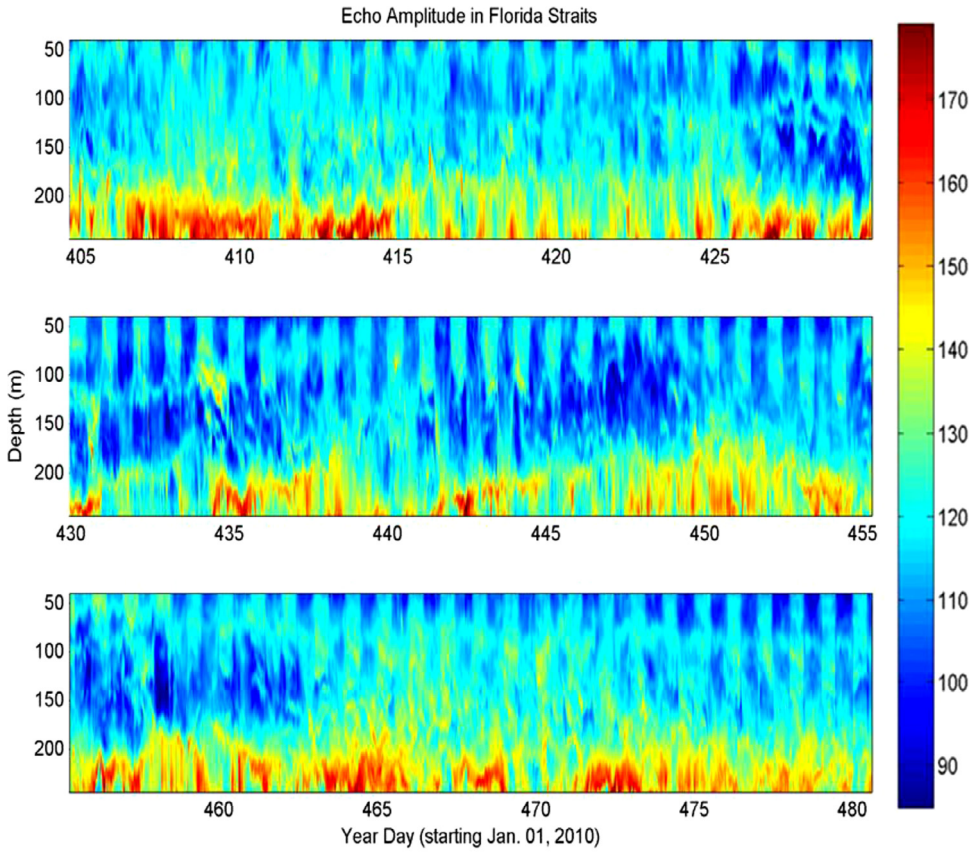

Fig. 4. Acoustic backscatter from bottom mounted ADCP for a subset of the 11 month data set from February 9, 2011 to April, 26, 2011.

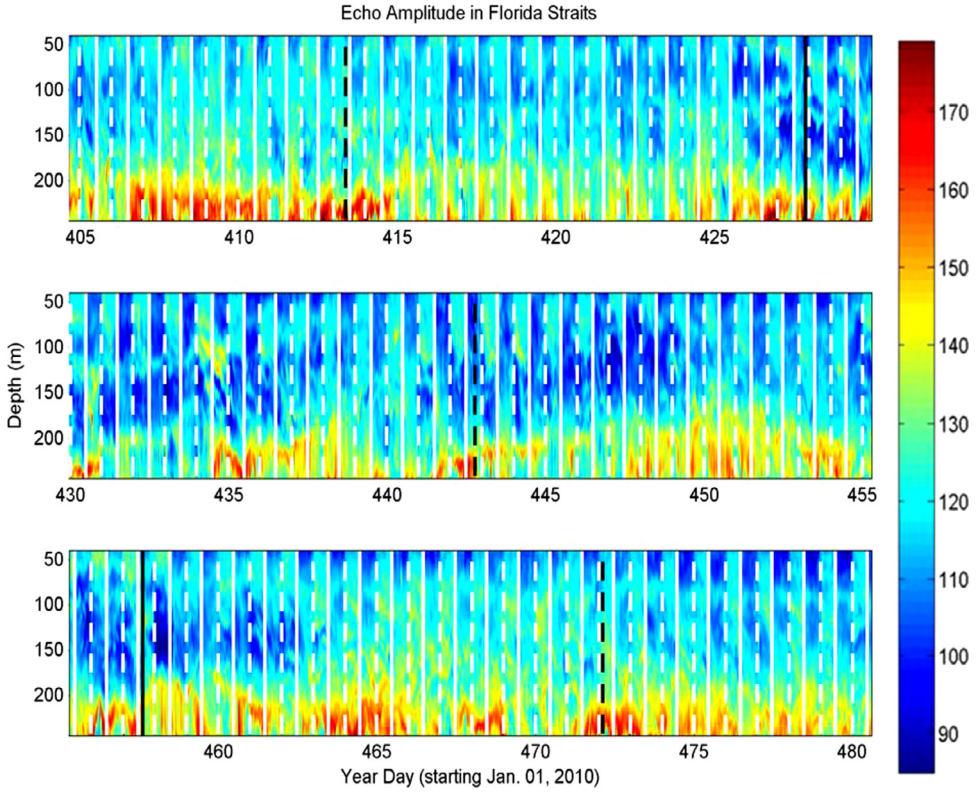

Fig. 5. Acoustic backscatter from bottom mounted ADCP for a subset of the 11 month data set from February 9, 2011 to April, 26, 2011 with sunrise times indicated by a solid white line, sunset by a dashed white line, new moon by a solid black line and full moon by a dashed black line. Near surface bins have been removed due to multiple reflections.

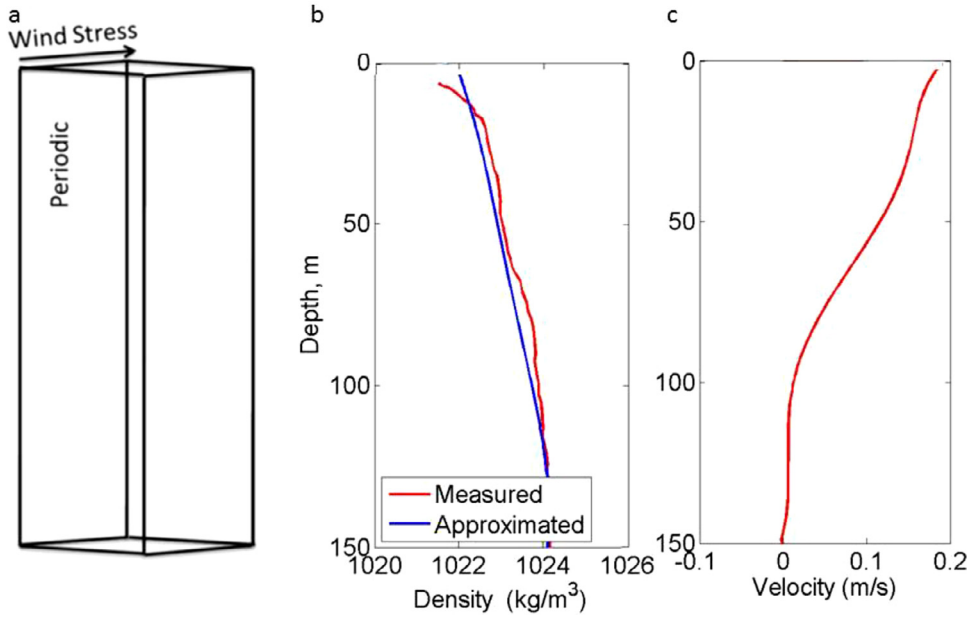

Fig. 6. Saanich Inlet model setup: (a) numerical domain; (b) measured potential density profile compared to the linearized average profile initiated in the model; (c) initial current velocity average profile.

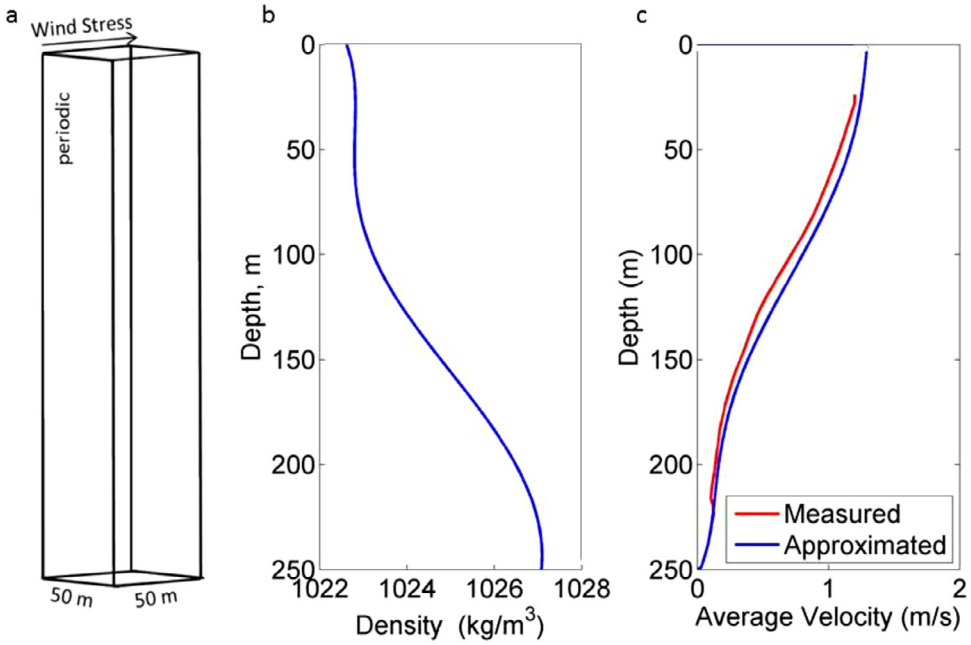

Fig. 7. Straits of Florida model setup: (a) numerical domain; (b) initial density profile; (c) measured current velocity profile compared to the linearized average profile initiated in the model.

simulation. In the implemented coupled mode, the particles and flow develop together in time and the effects of particles influence the flow solution and interact with the continuous phase. The particles were tracked and the solution was updated every two continuous phase iterations while the particle source term was recalculated every iteration. Dispersion of particles due to turbulence in the fluid phase was predicted using stochastic tracking and discrete random walk model. These models include the effect of instantaneous turbulent velocity fluctuations on the particle trajectories. DVM patterns may also involve collective behavior and other effects, which are not described by our model (see Section 5 for details).

In Saanich Inlet, concentrations of the dominating zooplankton (*Euphausia pacifica*) can range from 10 to 10,000 individuals/m^3 (Greenlaw, 1979; Mackie and Mills, 1983). Based on limited net samples collected 20 miles downstream from the ADCP mooring location, (USCG, 2008) concentrations of zooplankton in the Straits of Florida can vary significantly over time and species but are typically lower than in Saanich Inlet. To test what concentration of zooplankton is necessary to cause a measurable increase in turbulence, three different masses of particles were injected into the CFD model. The masses were determined by converting zooplankton concentrations to a mass of particles injected during one second time step, utilizing several simplifying assumptions. Based on data provided in

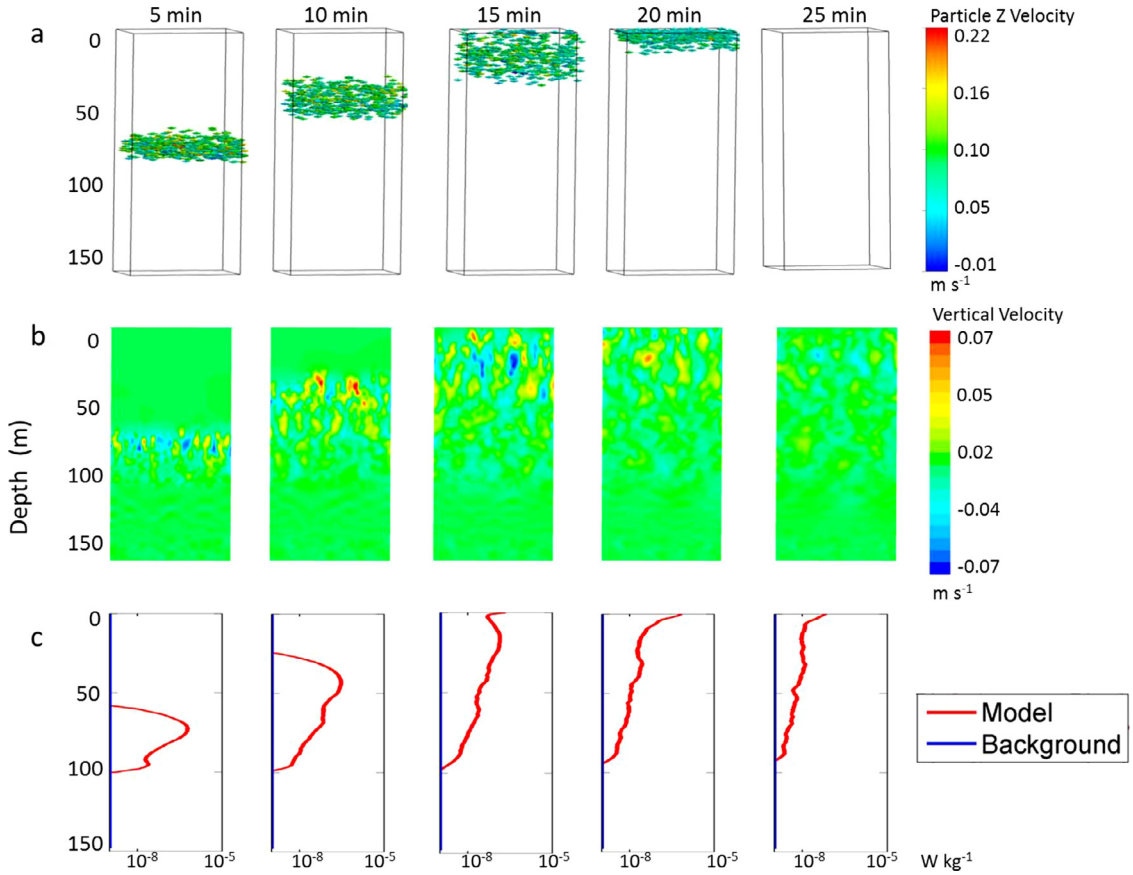

Fig. 8. Modelling the turbulence produced by DVM of zooplankton in Saanich Inlet by injecting 10,000 m^{-3} positively buoyant particles with 0.01 m diameter at 100 m: (a) particle locations at five minute intervals; (b) contours of vertical velocity; (c) average profiles of dissipation rate ε (W kg^{-1}). Background turbulence dissipation rate in Saanich Inlet is set at 10^{-9} W kg^{-1} following measurements by Kunze et al. (2006). In the upper few meters dissipation rate exceeded 10^{-9} W kg^{-1} due to surface wind stress and has been removed.

De Robertis et al. (2000), we assumed that organisms were spherical particles with radius $r = 0.005$ m and density ρ_o close to that of water. The estimated mass of particles to be injected into the model domain at the initial moment was calculated as follows:

$$\Delta M = \frac{4}{3}\pi r^3 c V \rho_0$$

where $V = \Delta z h^2$ is the volume of our numerical domain corresponding to the thickness $\Delta z = 25$ m of the zooplankton layer prior to migration reported by Kunze et al. (2006) and $h = 50$ m, the size of the domain in both horizontal dimensions. We tested extreme ($c = 10{,}000$ individuals/m^3), intermediate ($c = 5000$ individuals/m^3), and low ($c = 1000$ individuals/m^3) concentrations, which corresponded to injected mass of particles 3.27×10^5 kg, 1.635×10^5 kg, and 3.27×10^4 kg into the 1 m thick horizontal layer, respectively.

Boundary conditions for the DPM determine the trajectory of the particles after interaction with a boundary. The DPM boundary conditions at the top and bottom of the numerical domain were set to allow the particles to escape and side boundaries were set to reflect particles. The inlet was a periodic boundary, so particles flowed out one side of the domain and back into the other side with the fluid flow.

First, a spin up with no particles was run for 1440 steps (2 h). All cases were run with a 5 s time step with maximum 50 iterations per time step. After spin up, two separate cases were run for 420 steps (35 min), one with particles representing zooplankton and one without particles, for comparison of the respective velocity profiles. In this work, however, we did not intend to reproduce the background turbulence fields in Saanich Inlet and the Straits of Florida with a numerical model. For comparison with the turbulence produced by DVM, we used the background turbulence dissipation levels previously reported by Kunze et al. (2006) and Gregg et al. (1999) as 10^{-9} W kg^{-1} and 10^{-8} W kg^{-1}, respectively.

The LES WALE turbulence model does not directly output ε. Estimation of ε was made from the modeled turbulent velocity gradients in three directions as follows (Delafosse et al., 2008).

$$\varepsilon = 2(\nu_T + \nu)S_{ij}S_{ij} = \frac{\nu_T + \nu}{2}\left(\frac{\partial u_i}{\partial x_j} + \frac{\partial u_j}{\partial x_i}\right)^2 \quad (1)$$

Partial derivatives $\frac{\partial u_i}{\partial x_j}$ and $\frac{\partial u_j}{\partial x_i}$ are produced by the model. Subgrid turbulent viscosity ν_T is exported from the model; and, ν is the molecular viscosity of water, which is constant (10^{-6} m^2 s^{-1}).

Eq. (1) contains filtered turbulent velocity gradients, which are explicitly calculated in the LES model, and the turbulent viscosity calculated from the subgrid-scale model. The subgrid-scale model accounts for turbulence production by the particles. The subgrid-scale turbulence due to moving particles is therefore correctly represented in Eq. (1). This has been validated by the grid convergence test mentioned at the beginning of this section.

4. Results

Model runs with three different concentrations of particles and no particles have been analyzed for both Saanich Inlet and the Straits of Florida. In Saanich Inlet, the case with extreme concentration of particles (10,000 individuals/m^3) showed an increase in ε by approximately 2–3 orders of magnitude over background turbulence dissipation rate when particles, a proxy for migrating zooplankton,

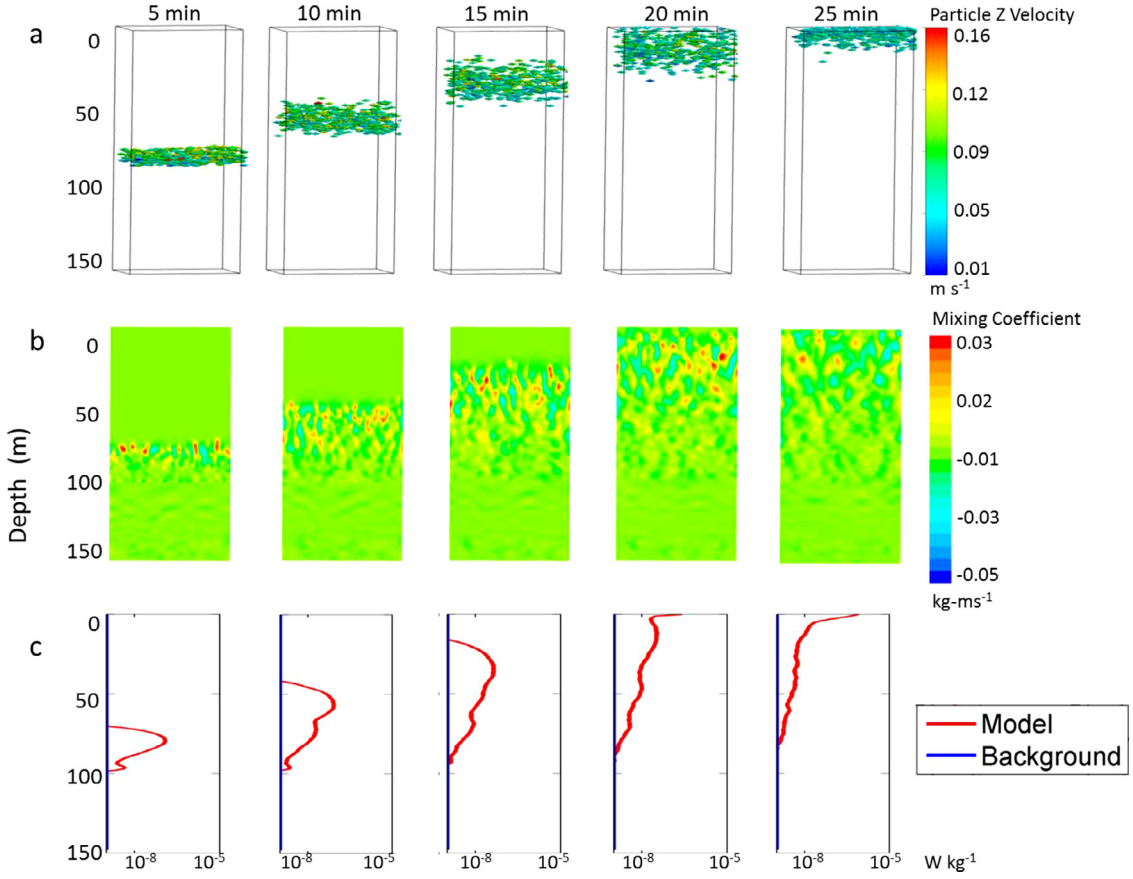

Fig. 9. Same as in Fig. 8, but by injecting 5000 particles m^{-3}.

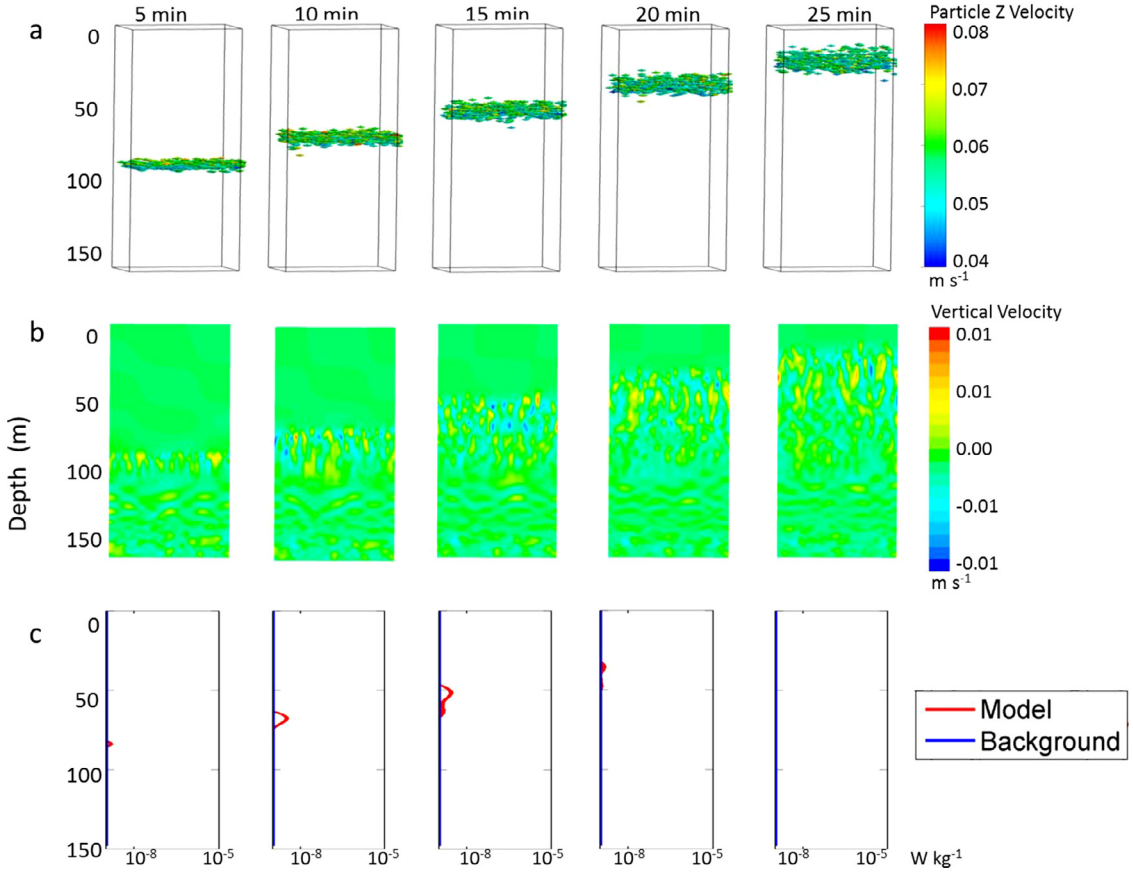

Fig. 10. Same as in Fig. 8, but by injecting 1000 particles m^{-3}.

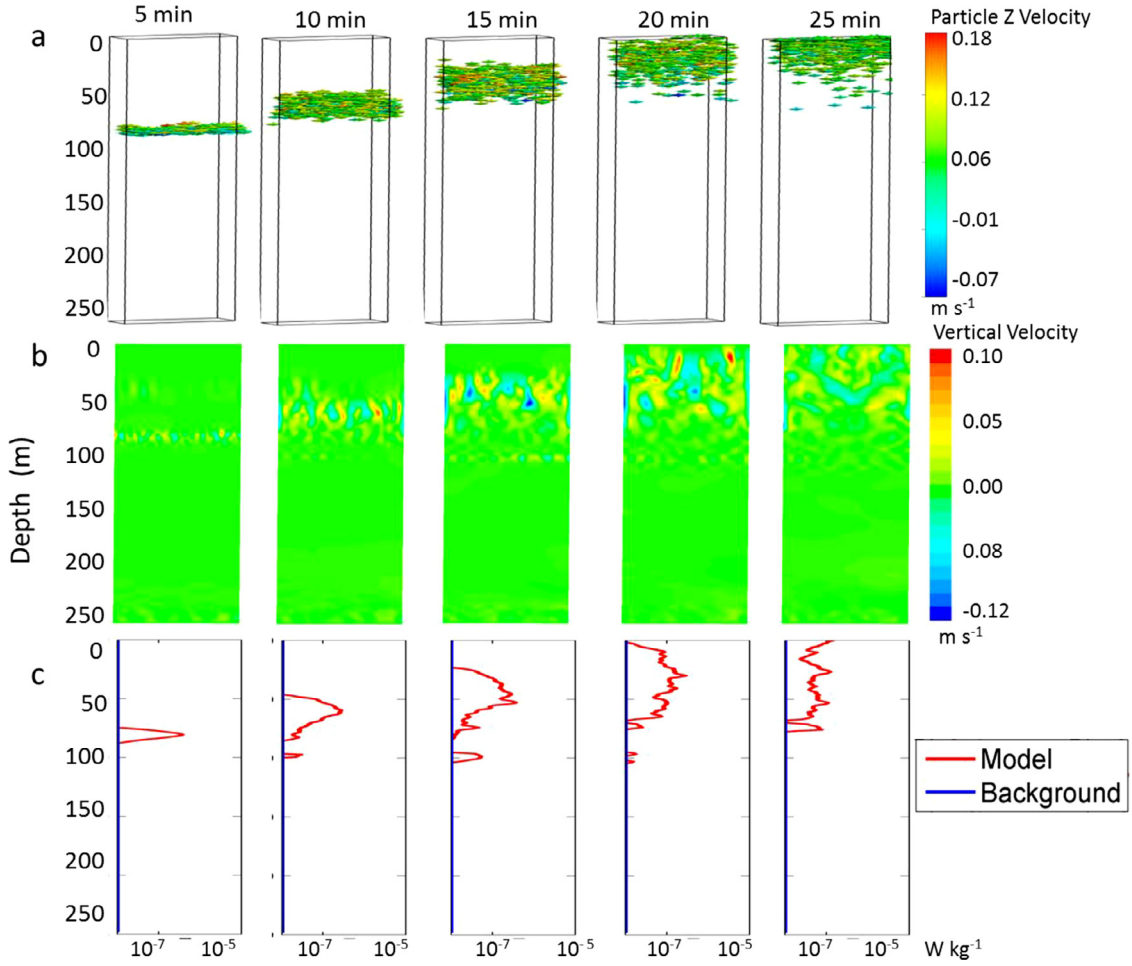

Fig. 11. Modeling turbulence produced by DVM of zooplankton in the Straits of Florida by injecting 10,000 positively buoyant particles m^{-3} with 0.01 m diameter at 100 m: (a) particle locations at five minute intervals; (b) contour plots of vertical velocity; (c) average profiles of dissipation rate ε (W kg^{-1}). Background turbulence dissipation rate in the Straits of Florida is set at 10^{-8} W kg^{-1} following measurements by Gregg et al. (1999). In the upper few meters dissipation rate exceeded 10^{-8} W kg^{-1} due to surface wind stress and has been removed.

were present in the mixed layer (Fig. 8). The background dissipation rate of turbulence was reported in Kunze et al. (2006) on the order of 10^{-9} W kg^{-1}. The turbulence induced by the particles remains in the wake of the particles for some time after they have migrated out of the area, which is seen on the vertical velocity contour plots (Fig. 8). The case with an intermediate concentration of particles (5000 individuals/m^3) showed an increase in ε of approximately 1–2 orders of magnitude during particle migration (Fig. 9). There is also an increase of turbulence in the wake of the particles, but it is less pronounced than at the extreme concentration of particles (Fig. 9). The case with low concentration of particles (1000 individuals/m^3) showed almost no change in ε over background turbulence during particle migration; though, there were still relatively small fluctuations of vertical velocity on the contour plots (Fig. 10). Note that the background turbulence dissipation rate in the model without particles was comparable or lower than the measurement noise reported by Kunze et al. (2006).

In the Straits of Florida case, the extreme concentration of particles (10,000 individuals/m^3) showed an increase in ε of approximately 1–2 orders of magnitude over background turbulence during particle migration (Fig. 11c).The background dissipation rate of turbulence was reported in Gregg et al. (1999) on the order of 10^{-8} W kg^{-1}. The turbulence induced by the particles remains in the wake of the particles for some time after they have migrated out of the area, but the signal was less pronounced than in the Saanich Inlet case (Fig. 11). The case with an intermediate concentration of particles (5000 individuals/m^3) showed an increase in ε of approximately 1–2 orders of magnitude over background turbulence during particle migration (Fig. 12). The case with a low concentration of particles (1000 individuals/m^3) showed approximately 1 order of magnitude change in ε over background turbulence during particle migration (Fig. 13).

The model results for the Straits of Florida were compared with the corresponding field data on the current velocity profiles. Profiles of northward current velocity were averaged over all sunrise and sunset times for the complete 11-month ADCP data set in cases within the Florida Current. We averaged only the current velocity profiles with maximum northward velocity component exceeding 0.75 m s^{-1} to be sure the data were within the Florida Current, because coastal waters may have different DVM patterns, in particular, due to freshwater influx, and, correspondingly, involve different biophysical interactions. The sunset/sunrise averaged profile was compared to the averaged profile three hours prior to migration of zooplankton. There was a slight, but statistically significant decrease in the northward component of velocity in the top 100 m during migrations as compared to three hours prior (Fig. 14). There is, however, evidence of velocity bias in ADCP data from self-propelled particles (Wilson and Firing, 1992; Smyth et al., 2006). However, during DVM the net propagation of zooplankton is in the vertical, rather than horizontal, direction and is not expected to significantly affect the ADCP current

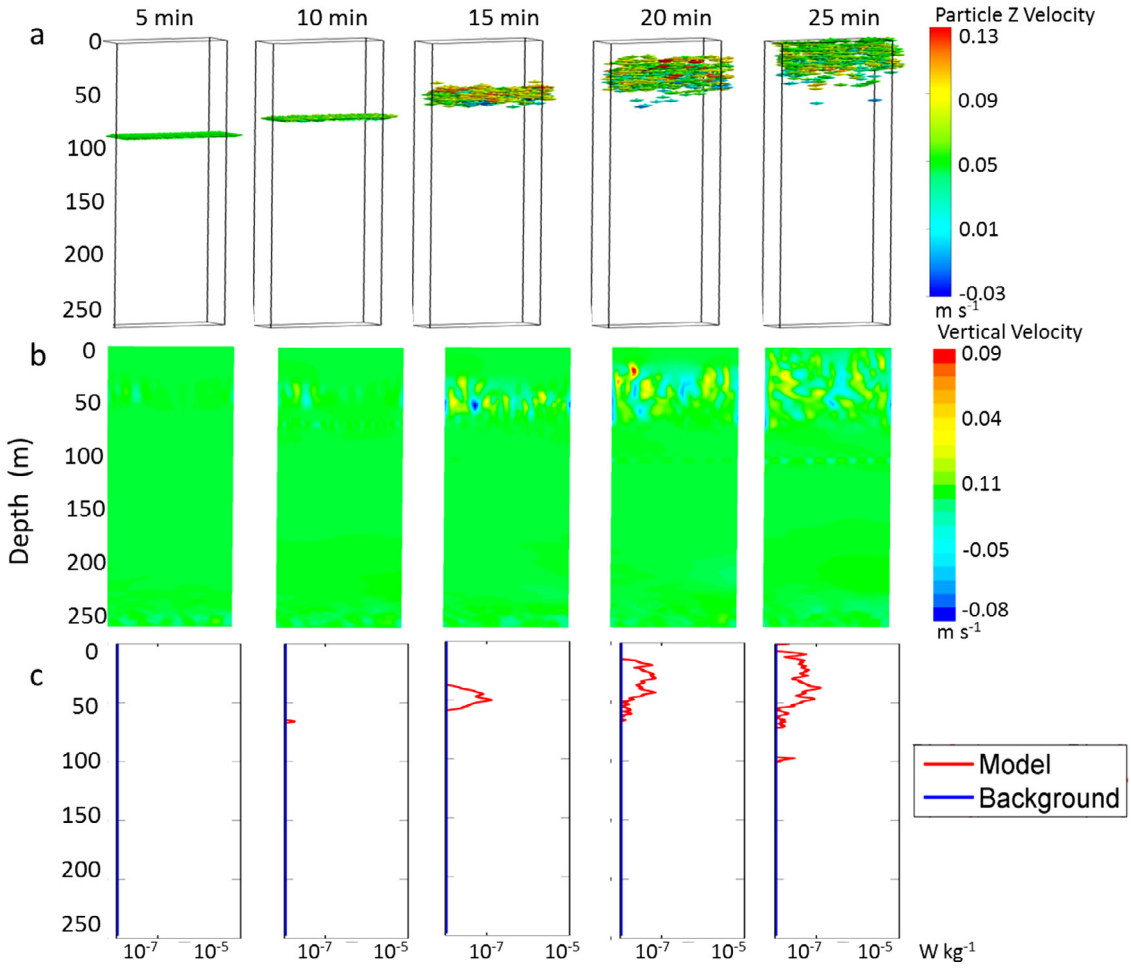

Fig. 12. Same as in Fig. 11, but by injecting 5000 particles m^{-3}.

velocity measurements. According to Smyth et al. (2006), horizontal velocities arising due to organisms swimming horizontally is generally absent from ADCP data, which has been attributed to uncorrelated horizontal motions among the scattering organisms (Geyer and Signell, 1990; Ott, 2005).

Both particle and no particle cases for the Straits of Florida are shown in Figs. 15 and 16. The average northward component of the velocity profile near the top of the model domain showed some decrease when an extreme and intermediate (not shown) concentration of particles was released (Fig. 15). These profiles were taken 25 min (300 steps) after the particles were released into the domain. The observational data also show a similar decrease (Fig. 14). The case with low concentrations of particles, 1000 individuals/m^3, (Fig. 16) showed a small change in simulated velocity profiles over the background velocity profiles with no particles.

5. Discussion

The numerical simulations conducted for Saanich Inlet suggest that DVM of zooplankton could cause a measurable increase of ε in the upper layer of the ocean. Kunze et al. (2006) reported an increase of instantaneous ε, presumably due to DVM, up to 5 orders of magnitude. Our model produces an increase of ε up to 2–3 orders of magnitude over background turbulence. The difference can be explained by the fact that Kunze et al. (2006) measured instantaneous profiles of ε, while the model results on ε in Figs. 8–13 are averaged horizontally over the 50 m by 50 m domain.

In the simulation for the Straits of Florida for all three concentrations of particles, ε was consistent with those for Saanich Inlet, though some differences of an order of magnitude took place. The difference in ε produced by the model for Saanich Inlet and the Straits of Florida is mostly due to the difference in stratification. This result indicates that the impact of DVM on turbulent mixing is apparently dependent on the concentration of zooplankton undergoing migration and stratification. In Saanich Inlet, concentrations of zooplankton are known to range between 10 and 10,000 organisms/m^3. According to available data on concentrations of zooplankton in the Straits of Florida, concentrations are on the lower limit of those reported for Saanich Inlet. At a low concentration, the model indicates there should be no significant impact on turbulence. Assigning the properties of migrating zooplankton to buoyant spherical particles, however, might result in the overestimation or underestimation of turbulence levels in our model. Using buoyant spherical particles as a proxy for swimming zooplankton could result in an overestimate of turbulence production, because the drag coefficient for a sphere is an order of magnitude greater than a streamlined body, which many zooplankton possess. Self-propelled zooplankton have been known to cause an increase in turbulence on time scales smaller than a few minutes and length scales of a couple of body lengths (Cheng and Chahine, 2001; Videler et al., 2002; Yen et al., 2003; Catton et al., 2011). It is, therefore, also possible that the level of increase of turbulence by swimming zooplankton, predicted in our model, is an underestimate. Because of the low propulsive efficiency of zooplankton, from 0.1 to 0.3, much energy is expended to overcome the drag of the water, creating additional turbulence (Huntley and Zhou, 2004). Swimming

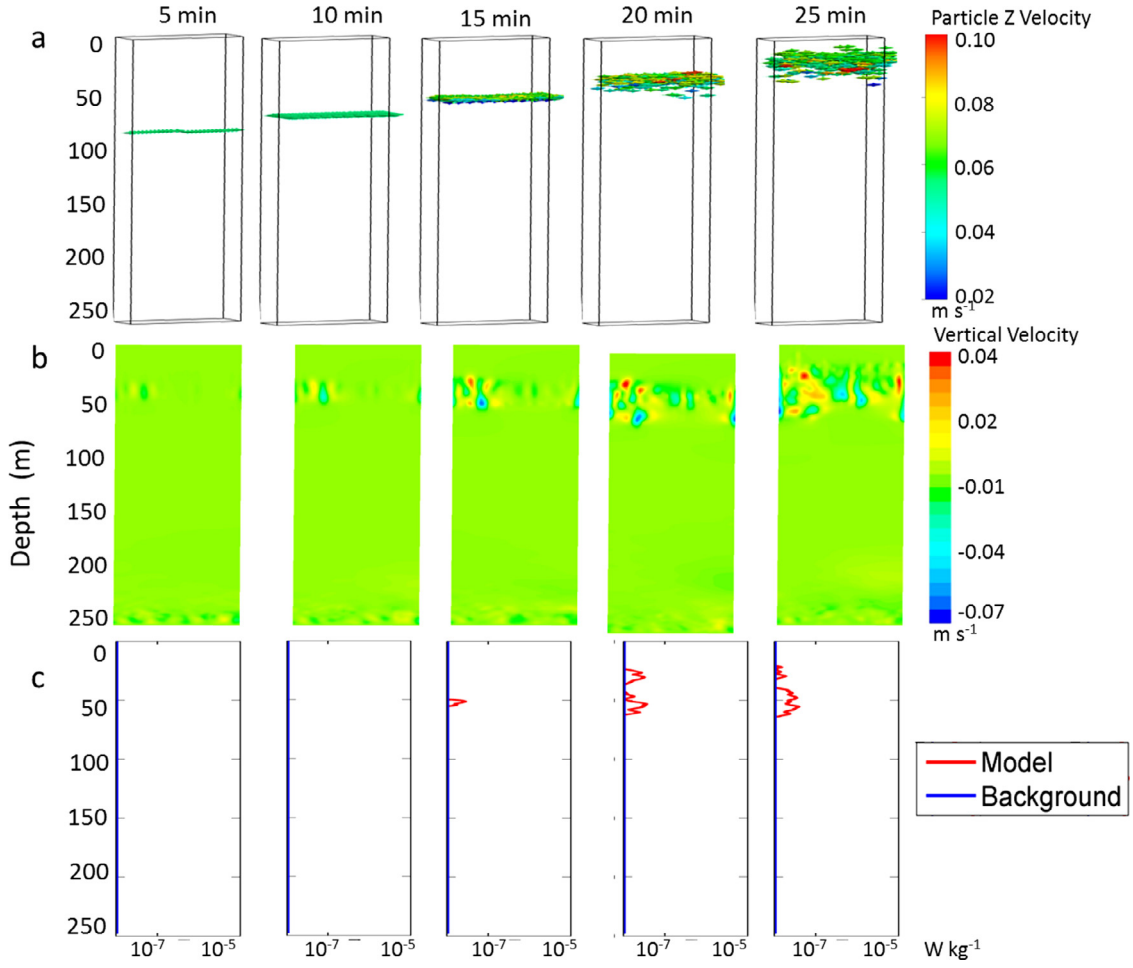

Fig. 13. Same as in Fig. 11, but by injecting 1000 particles m^{-3}.

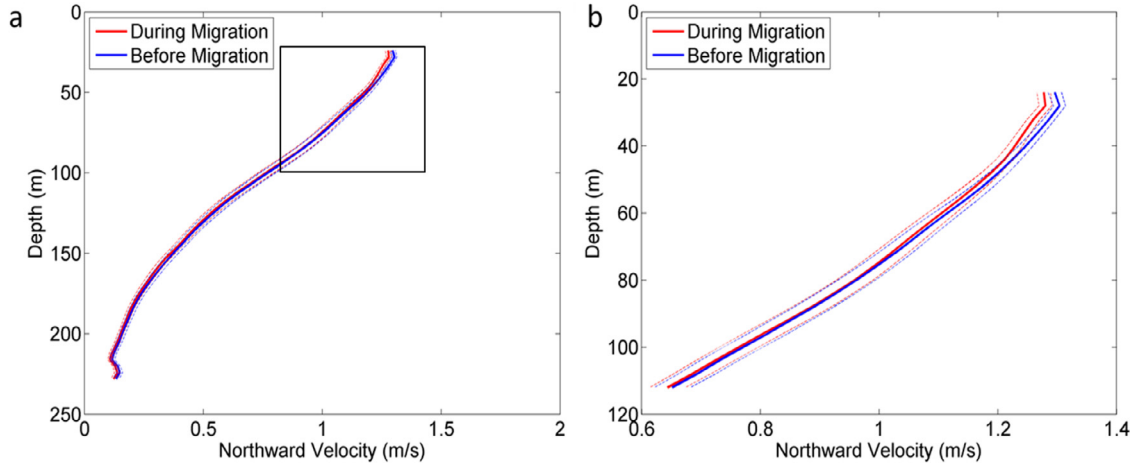

Fig. 14. Average current velocity in full 11 month data set northward current velocity profiles of sunrise/sunset compared to three hours prior using a 95% confidence interval (represented by dotted lines) from ADCP: (a) complete average velocity profile; (b) top 110 m of the profile.

zooplankton have been shown in laboratory experiments in a non-stratified tank (Wilhelmus and Dabiri, 2014) to create intermittent jets that have Kelvin–Helmholtz instabilities significantly larger than the size of individuals. If this behavior was taken into account, the increase of turbulence in our model could take place at lower concentrations of zooplankton. The efficiency of mixing depends on the scale of generated turbulence relative to vertical buoyancy scale. With increasing length scale of generated turbulence, the mixing efficiency increases (Kunze, 2011). The mixing efficiency depends on the ratio of the length scale of generated turbulence to vertical buoyancy scale (Visser, 2007). In addition, the use of spherical particles apparently oversimplified the effect of collective behavior on turbulence generation, which depends on the volume and concentration of the organisms as well as their shape and orientation (Katija, 2012).

Unfortunately, the environmental conditions in Saanich Inlet and the Straits of Florida were not completely known. Knowing exact

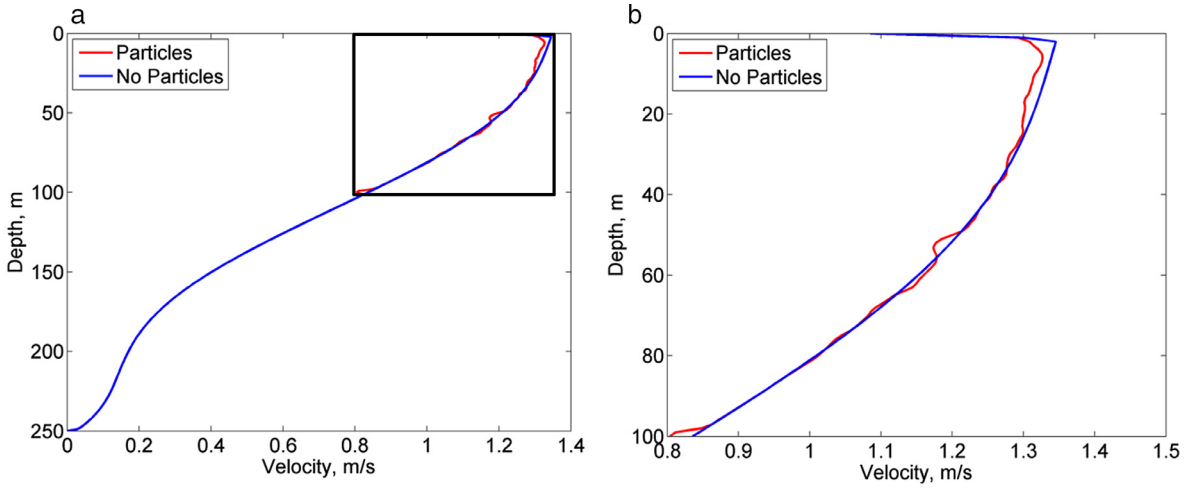

Fig. 15. Average current velocity in Straits of Florida model with extreme concentration of particles: (a) full domain; (b) top 110 m.

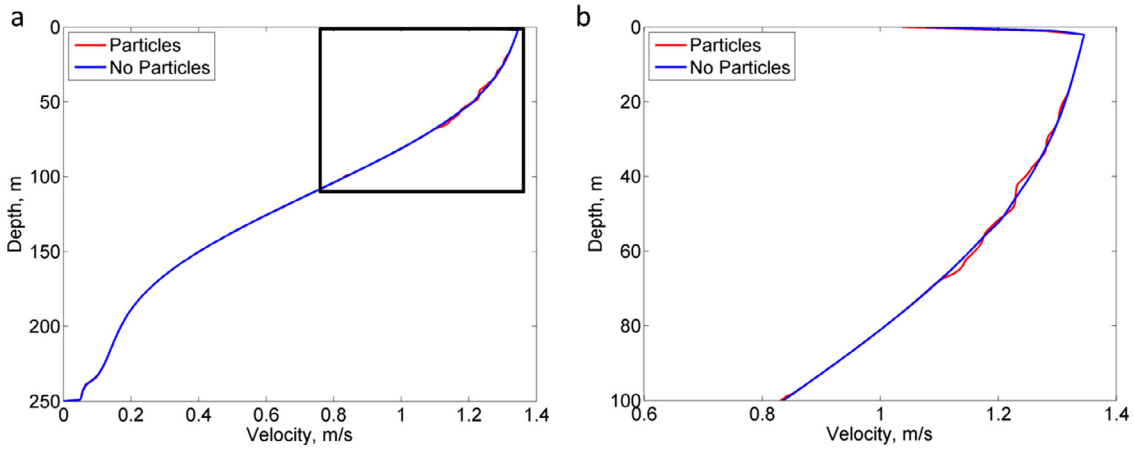

Fig. 16. Average current velocity in Straits of Florida model with low concentration of particles: (a) full domain; (b) top 110 m.

temperature, salinity, and velocity profiles in Saanich Inlet at the time of sampling would have been beneficial to accurately set the model and recreate the increase of ε observed by Kunze et al. (2006). For the Straits of Florida case, velocity profiles were taken from ADCP measurements; however, in this highly energetic area there are many changes to the current velocity over different time scales. Based on observation, but a still largely idealized temperature profile was used to initialize the model for the Straits of Florida.

A relatively small, but measurable and statistically significant, decrease in the northward current velocity of the Florida Current near the surface can be linked to the presence of zooplankton or small fish undergoing a DVM cycle when averaged over the 11-month ADCP data set (Fig. 14). (Note the near surface bins had to be removed due to multiple reflections.) This decrease in current velocity was reproduced in the model (Fig. 15) and was due to the change of the vertical mixing coefficient produced by additional turbulence from a large mass of zooplankton moving into or out of the area. Increased turbulent friction caused drag, reducing the northward current velocity. Note that DVM takes place in less than 1 h, and its effect on the current velocity profiles can be classified as an ageostrophic process. Comparison of the model and average ADCP velocity profiles is of course complicated by their substantial dependence on the environmental conditions, not directly related to DVM, including wind-wave mixing, Florida Current meandering, and tides. In principle, diurnal cycles, breezes, and tides can have an effect on the velocity field even at 20–30 m depth. We have performed a test by reducing the averaging interval from ± 1 h to ± 0.5 h around sunset/sunrise and 3–4 h prior and there was no statistically significant change in the velocity profiles averaged over 11 months. This is an indication that diurnal cycle, breezes, and tides did not affect the averaged velocity profiles in any significant way (though they could affect individual sunrise/sunset velocity profiles).

6. Conclusions

There has been much debate on the topic of biomixing and its impact on global ocean circulation, but details are still not completely clear. The computational fluid dynamics model in our work was able to reproduce an increase in ε due to DVM. Our model indicates that the impact of DVM on ε is largely dependent on the concentration of zooplankton undergoing migration. In Saanich Inlet, concentrations of zooplankton are known to be high enough at certain times of the year, which could produce measurable turbulence as predicted by the model. However, concentrations of zooplankton are highly variable, which may explain why subsequent studies of bioturbulence in Saanich Inlet did not show an increase of ε (Rousseau et al., 2010). Unfortunately, there were no measurements of zooplankton concentration in Saanich Inlet during either the Kunze et al. (2006) or Rousseau et al. (2010) experiments.

Our model also shows that even in a highly energetic environment, such as the Straits of Florida, it is possible for a sufficiently large concentration of zooplankton undergoing DVM to increase turbulence over background level. As our measurements and model results show, the increase of vertical mixing could even affect the current velocity profile during DVM. However, there are many other environmental processes not directly related to DVM such as wind-wave

mixing, diurnal cycles, Florida Current meandering, and tides, which can have a much larger impact on the current velocity.

On one hand, using buoyant spherical particles as a proxy for swimming zooplankton could result in an overestimate of turbulence production because the drag coefficient for a sphere is an order of magnitude greater than a streamlined body, which many zooplankton possess. On the other hand, self-propulsion of zooplankton may significantly increase turbulence generation compared to the rigid spherical particles used in this study as a proxy for zooplankton. This means that bioturbulence can be significant even at low concentrations of zooplankton. In fact, "Observations of laser-induced vertical migrations of *Artemia salina* reveal the appearance of a downward jet, which triggers a Kelvin–Helmholtz instability that results in the generation of eddy-like structures with characteristic length scales much larger than the organisms" (Wilhelmus and Dabiri, 2014).

While our model does show an increase in turbulence during DVM of a sufficiently large mass of zooplankton, actual conditions in the ocean can vary dramatically. The strength of DVM is dependent on many factors such as on geographic location, season, cloud cover, lunar cycle, density of organisms, etc. The mixing efficiency of the migrating zooplankton depends on the ratio of the length scale of generated turbulence to vertical buoyancy scale (Visser, 2007); while, the later also varies significantly in the ocean. Moreover, anthropogenic pollutants such as oil spills and dispersants may also affect behavioral patterns of zooplankton, including DVM, with largely unknown but possibly dramatic, or even lethal, effects on marine ecosystems.

Acknowledgments

We give a special thanks to Dr. Eric Kunze for helpful comments on this work. We acknowledge the GoMRI project "Consortium for the Advanced Research on Transport of Hydrocarbons in the Environment" (PI: Tamay Özgökomen, UM RSMAS) for support for analysis of this data. Data collection by NSUOC was funded by ONR, Award N00014-10-1-0938.

Appendix

The filtered time-dependent Navier–Stokes equations (Eqs. (1)–(4)) are as follows:

$$\frac{\partial \rho}{\partial t} + \frac{\partial}{\partial x_i}(\rho \bar{u}_i) = 0 \tag{1}$$

$$\frac{\partial}{\partial t}(\rho \bar{u}_i) + \frac{\partial}{\partial x_j}\left(\rho \bar{u}_i \bar{u}_j\right) = \frac{\partial}{\partial x_j}\left(\sigma_{ij}\right) - \frac{\partial \bar{\rho}}{\partial x_i} - \frac{\partial \tau_{ij}}{\partial x_j} \tag{2}$$

where σ_{ij} is the stress tensor due to molecular viscosity defined by

$$\sigma_{ij} = \left[\mu\left(\frac{\partial \bar{u}_i}{\partial x_j} + \frac{\partial \bar{u}_j}{\partial x_i}\right)\right] - \frac{2}{3}\mu \frac{\partial u_i}{\partial x_i}\delta_{ij} \tag{3}$$

and τ_{ij} is the subgrid-scale stress defined by

$$\tau_{ij} = \rho u_i u_j - \rho \bar{u}_i \bar{u}_j \tag{4}$$

In the WALE model (Nicoud and Ducros, 1999) the eddy viscosity was modeled by:

$$\mu_t = \rho L_s^2 \frac{\left(S_{ij}^d S_{ij}^d\right)^{3/2}}{\left(\bar{S}_{ij}\bar{S}_{ij}\right)^{5/2} + \left(S_{ij}^d S_{ij}^d\right)^{5/4}} \tag{5}$$

where L_s and S_{ij}^d in the WALE model are defined, respectively as

$$L_s = \min\left(xd, C_w V^{1/3}\right) \tag{6}$$

$$S_{ij}^d = \frac{1}{2}\left(\bar{g}_{ij}^2 + \bar{g}_{ji}^2\right) - \frac{1}{3}\zeta_{ij}\bar{g}_{kk}^2, \bar{g}_{ij} = \frac{\delta \bar{u}_i}{\delta x_j} \tag{7}$$

In Fluent the default value of the WALE constant C_w is 0.325 (ANSYS *Fluent*, 2013).

References

Andersen, V., Nival, P., 1991. A model of the diel vertical migration of zooplankton based on euphausiids. J. Mar. Res. 49, 153–175.
Ansys Fluent 14.5 (2013), Fluent User's Guide. http://www.fluent.com/.
Carassou, L., Hernandez, F.J., Graham, W.M., 2014. Change and recovery of coastal mesozooplankton community structure during the Deepwater Horizon oil spill. Environ. Res. Lett. 9, 124003.
Catton, K.B., Webster, D.R., Kawaguchi, S., Yen, J., 2011. The hydrodynamic disturbances of two species of krill: implications for aggregation structure. J. Exp. Biol. 214, 1845–1856.
Cheng, J.Y., Chahine, G.L., 2001. Computational hydrodynamics of animal swimming: boundary element method and three-dimensional vortex wake structure. Comp. Biochem. Physiol. Part A: Mol. Integr. Physiol. 131, 51–60.
Cohen, J.H., McCormick, L.R., Burkhardt, S.M., 2014. Effects of dispersant and oil on survival and swimming activity in a marine copepod. Bull. Environ. Contam. Toxicol 92, 381–387.
Crone, T.J., Tolstoy, M., 2010. Magnitude of the 2010 Gulf of Mexico oil leak. Science 330, 634–643.
Dabiri, J.O., 2010. Role of vertical migration in biogenic ocean mixing. Geophys. Res. Lett. 37, L11602.
Delafosse, A., Line, A., Morchain, J., Guiraud, P., 2008. LES and URANS simulations of hydrodynamics in mixing tank: comparison to PIV experiments. Chem. Eng. Res. Des. 86, 1322–1330.
De Robertis, A., Jaffe, J.S., Ohman, M.D., 2000. Size-dependent visual predation risk and the timing of vertical migration in zooplankton. Limnol. Oceanogr. 45, 1838–1844.
De Robertis, A., Schell, C., Jaffe, J.S., 2003. Acoustic observations of the swimming behavior of the euphausiid *Euphausia pacifica* Hansen. ICES J. Mar. Sci. 60, 885–898.
Dewar, W.K., Bingham, R.J., Iverson, R.L., Nowacek, D.P., St. Laurent, L.C., Wiebe, P.H., 2006. Does the marine biosphere mix the ocean? J. Mar. Res. 64, 541–561.
Enright, J.T., 1977. Diurnal vertical migration: adaptive significance and timing. Part 1. Selective advantage: a metabolic model. Limnol. Oceanogr. 22, 856–872.
Geyer, W.R., Signell, R., 1990. Measurements of tidal flow around a headland with a shipboard acoustic Doppler current profiler. J. Geophys. Res. Oceans 95, 3189–3197.
Gliwicz, M.Z., 1986. Predation and the evolution of vertical migration in zooplankton. Nature 320, 746–748.
Greenlaw, C.F., 1979. Acoustical estimation of zooplankton populations. Limnol. Oceanogr. 24, 226–242.
Gregg, M., Winkel, D., MacKinnon, J., Lien, R., 1999. Mixing over shelves and slopes. In: Muller, P., Henderson, D. (Eds.), Dynamics of Oceanic Internal Gravity Waves II, Proceedings, Hawaiian Winter Workshop. DTIC Document, pp. 35–42.
Gregg, M.C., Horne, J.K., 2009. Turbulence, acoustic backscatter, and pelagic nekton in Monterey Bay. J. Phys. Oceanogr. 39, 1097–1114.
Haney, J.F., 1988. Diel patterns of zooplankton behavior. Bull. Mar. Sci. 43, 583–603.
Huntley, M.E., Zhou, M., 2004. Influence of animals on turbulence in the sea. Mar. Ecol. Prog. Ser. 273, 65–79.
Ianson, D., Jackson, G.A., Angel, M.V., Lampitt, R.S., Burd, A.B., 2004. Effect of net avoidance on estimates of diel vertical migration. Limnol. Oceanogr. 49, 2297–2303.
Jenkins, W.J., Doney, S.C., 2003. The subtropical nutrient spiral. Global Biogeochem. Cycles 17, 1110.
Katija, K., 2012. Biogenic inputs to ocean mixing. J. Exp. Biol. 215, 1040–1049.
Kunze, E., Dower, J.F., Beveridge, I., Dewey, R., Bartlett, K.P., 2006. Observations of biologically generated turbulence in a coastal inlet. Science 313, 1768–1770.
Kunze, E., Dower, J.F., Dewey, R., D'Asaro, E.A., 2007. Mixing it up with krill. Science 318, 1239 author reply 1239.
Kunze, E., 2011. Fluid mixing by swimming organisms in the low-Reynolds-number limit. J. Mar. Res 69, 591–601.
Lampert, W., 1989. The adaptive significance of diel vertical migration of zooplankton. Funct. Ecol. 3, 21–27.
MacKenzie, B.R., Leggett, W.C., 1993. Wind-based models for estimating the dissipation rates of turbulent energy in aquatic environments: empirical comparisons. Mar. Ecol. Prog. Ser. 94, 207–216.
Mackie, G.O., Mills, C.E., 1983. Use of the PICES IV submersible for zooplankton studies in coastal waters of British Columbia. Can. J. Fish. Aquat. Sci. 40, 763–776.
Morsi, S.A., Alexander, A.J., 1972. An investigation of particle trajectories in two-phase flow systems. J. Fluid Mech. 55, 193–208.
Munk, W.H., 1966. Abyssal recipes. Deep Sea Res. 13, 707–730.
Munk, W., Wunsch, C., 1998. Abyssal recipes II: energetics of tidal and wind mixing. Deep Sea Res. Part I: Oceanogr. Res. Pap. 45, 1977–2010.
Nicoud, F., Ducros, F., 1999. Subgrid-scale stress modelling based on the square of the velocity gradient tensor. Flow Turbul. Combust. 62, 183–200.
Ott, M.W., 2005. The accuracy of acoustic vertical velocity measurements: instrument biases and the effect of zooplankton migration. Cont. Shelf Res. 25, 243–257.
Pakhomov, E., Yamamura, O. 2010. Report of the advisory panel on micronekton sampling inter-calibration experiment. PICES Scientific Report No. 38. North Pacific Marine Science Organization (PICES), Sidney, BC.
Rousseau, S., Kunze, E., Dewey, R., Bartlett, K., Dower, J., 2010. On turbulence production by swimming marine organisms in the open ocean and coastal waters. J. Phys. Oceanogr. 40, 2107–2121.
Science Applications International Corporation, 1992. Straits of Florida Physical Oceanographic Field Study. Final Interpretative Report Volume II: Technical Report. U.S. Department of the Interior. Minerals Management Service, Atlantic OCS Regional Office.
Smyth, C., Hay, A.E., Hill, P.S., Schillinger, D., 2006. Acoustic observations of vertical and horizontal swimming velocities of a diel migrator. J. Mar. Res 64, 723–743.

St. Laurent, L., Simmons, H., 2006. Estimates of power consumed by mixing in the ocean interior. J. Clim. 19, 4877–4890.
Soloviev, A.V., Hirons, A., Maingot, C., Dodge, R.E., Yankovsky, A.E., Wood, J., Weisberg, R.H., Luther, M.E., McCreary, J.P., 2015. Submitted. Southward flow on the coastal flank of the Florida Current. Deep-Sea Res.
Stich, H.-B., Lampert, W., 1981. Predator evasion as an explanation of diurnal vertical migration by zooplankton. Nature 293, 396–398.
United States Coast Guard (USCG), 2008. Environmental impact statement for the Calypso LNG Deepwater Port license application, vols. 1 and 2, p. 1657.
Videler, J.J., Stamhuis, E.J., Müller, U.K., 2002. The scaling and structure of aquatic animal wakes. Integr. Comp. Biol. 42, 988–996.
Visser, A.W., 2007. Biomixing of the oceans? Science 316, 838–839.
Waterhouse, A.F., MacKinnon, J.A., Nash, J.D., Alford, M.H., Kunze, E., Simmons, H.L., Polzin, K.L., St. Laurent, L.C., Sun, O.M., Pinkel, R., Talley, L.D., Whalen, C.B., Huussen, T.N., Carter, G.S., Fer, I., Waterman, S., Naveira Garabato, A.C., Sanford, T.B., Lee, C.M., 2014. Global patterns of diapycnal mixing from measurements of the turbulent dissipation rate. J. Phys. Oceanogr. 44, 1854–1872.
Wilhelmus, M.M., Dabiri, J.O., 2014. Observations of large-scale fluid transport by laser-guided plankton aggregations. Phys. Fluids 26, 101302.
Wilson, C.D., Firing, E., 1992. Sunrise swimmers bias acoustic Doppler current profiles. Deep Sea Res. Part I: Oceanogr. Res. Pap. 39, 885–892.
Wunsch, C., Ferrari, R., 2004. Vertical mixing, energy, and the general circulation of the oceans. Annu. Rev. Fluid Mech. 36, 281–314.
Wunsch, C., 2000. Moon, tides and climate. Nature 405, 743–744.
Yen, J., Brown, J., Webster, D.R., 2003. Analysis of the flow field of the krill, *Euphausia pacifica*. Mar. Freshwater Behav. Physiol. 36, 307–319.